12th International Symposium on Turbulence and Shear Flow Phenomena (TSFP12)
Osaka, Japan (Online), July 19-22, 2022

A NEW POINT OF VIEW ON SKIN-FRICTION CONTRIBUTIONS IN ADVERSE-PRESSURE-GRADIENT TURBULENT BOUNDARY LAYERS

Marco Atzori
Department of Particulate Flow Modelling
Johannes Kepler University
4040 Linz, Austria
marco.atzori@jku.at

Alexander Stroh & Davide Gatti
Institute of Fluid Mechanics (ISTM)
Karlsruhe Institute of Technology
76131 Karlsruhe, Germany

Koji Fukagata
Department of Mechanical Engineering
Keio University
223-8522 Yokohama, Japan

Ricardo Vinuesa & Philipp Schlatter
SimEx/FLOW, Engineering Mechanics
KTH Royal Institute of Technology
100 44 Stockholm, Sweden

ABSTRACT

Skin-friction decompositions such as the so-called FIK identity (Fukagata *et al.*, 2002) are useful tools in identifying relevant contributions to the friction, but may also lead to results difficult to interpret when the total friction is recovered from cancellation of multiple terms with large values. We propose a new formulation of the FIK contributions related to streamwise inhomogeneity, which is derived from the convective form of the momentum equation and using the concept of dynamic pressure. We examine turbulent boundary layers subjected to various pressure-gradient conditions, including cases with drag-reducing control. The new formulation distinguishes more precisely the roles of the free-stream pressure distribution, wall-normal convection, and turbulent fluctuations. Our results allow to identify different regimes in adverse-pressure-gradient turbulent boundary layers, corresponding to different proportions of the various contributions, and suggest a possible direction towards studying the onset of mean separation.

INTRODUCTION

The skin-friction coefficient, denoted by $c_f = 2\tau_w/(\rho U_\infty^2)$, is a key physical quantity in wall-bounded flows. In this expression, the wall-shear stress is $\tau_w = \rho\nu(\mathrm{d}U_t/\mathrm{d}y_n)_{y_n=0}$, and $(1/2)\rho U_\infty^2$ is the dynamic pressure in the free stream. The subscripts t and n denote the wall-tangential and wall-normal directions, respectively. Hereafter, mean quantities and fluctuations are defined according to the Reynolds decomposition $\tilde{u} = U + u$, where the averaging operator is $U = \bar{\tilde{u}}$. Various identities that express c_f as a combination of different contributions have been derived, with the aim of explaining the mechanisms that generate friction. One example is the so-called FIK identity (Fukagata *et al.*, 2002), which is the focus of the present paper. The results are relatively straightforward for canonical flows such as periodic pipes and channels, where most of terms in the mean governing equations vanish. However, in more complex turbulent flows, skin-friction decompositions can lead to many contributions of much higher values than the total c_f, which makes it more challenging to identify the most relevant phenomena. Turbulent boundary layers (TBLs) subjected to strong adverse pressure gradients (APGs) are one of such cases. The appearance of many contributions with high values can also become problematic in describing control effects. The skin-friction reduction due to uniform blowing and skin-friction increase due to suction are convincingly explained by the turbulent-fluctuation contribution on ZPG TBL (Kametani *et al.*, 2015). When control is applied on the intense APG TBL developing over a wing section, however, many terms are significantly impacted (Atzori *et al.*, 2021). A similar outcome is also obtained using the RD decomposition (Renard & Deck, 2016), as shown by Fan *et al.* (2022) on wing boundary layers with control. The RD decomposition is derived to obtain better scaling than the FIK identity when the contributions are expressed in inner units, but the increase of many relevant terms in cases that are not homogeneous in the streamwise direction remains an issue. The aim of the present paper is to derive an alternative form of the FIK identity that can provide results with easier interpretation in case of strongly non-homogeneous flows.

DATA SET

We focus on the high-resolution large-eddy-simulation (LES) data sets for ZPG and APG TBLs over flat plate presented by Eitel-Amor *et al.* (2014) and Bobke *et al.* (2017), respectively, to describe pressure-gradient effects. These simulations were performed using the spectral code SIMSON (Chevalier *et al.*, 2007). High-resolution LESs of the flow around a NACA4412 airfoil at a Reynolds number based on the chord length of $Re_c = 400,000$ and angle of attack 5 degrees, including the case with uniform blowing for drag reduction (Vinuesa *et al.*, 2018; Atzori *et al.*, 2021), are also considered to describe control effects. These simulations were performed using the spectral-element code Nek5000 (Fischer *et al.*, 2008). In both cases, the LES filter is based on the relaxation-term approach described by Schlatter *et al.* (2004). In the airfoil simulations, only a portion of the suction side is considered in the present study, namely between $x/c = 0.24$ and $x/c = 0.86$, where uniform blowing is applied in the control case (note that x/c is the distance from the leading edge

Table 1. Range of pressure-gradient parameter (β), Reynolds number based on the momentum thickness (Re_θ), and friction Reynolds number (Re_τ) in the considered data set. Note that WSS and WSSB denote a portion of the wing suction side without and with uniform blowing, respectively.

Case	β	Re_θ	Re_τ
ZPG	≈ 0	$[541, 2272]$	$[218, 780]$
APG1	$[0.2, 1, 1]$	$[556, 3249]$	$[222, 798]$
APG2	$[0.3, 1.6]$	$[569, 3400]$	$[221, 827]$
WSS	$[0.1, 9.6]$	$[450, 2155]$	$[179, 363]$
WSSB	$[0.1, 17]$	$[450, 2455]$	$[175, 335]$

measured on the chord, normalised with the chord length).

The following relevant boundary-layer parameters are reported in Table 1 for all cases examined in the paper. The Clauser pressure-gradient parameter (Clauser, 1956) is computed as $\beta = \delta^*/\tau_w \mathrm{d}P/\mathrm{d}x_t|_e$. In this expression, δ^* is the displacement thickness, and $\mathrm{d}P/\mathrm{d}x_t|_e$ is the pressure gradient at $y_n = \delta_{99}$, where δ_{99} is the location of edge velocity. The value of U_e, and thus δ_{99}, δ^* and θ, are evaluated consistently for the entire data set using the method based on the diagnostic scaling proposed by Vinuesa *et al.* (2016). The Reynolds number based on the momentum thickness is defined as $Re_\theta = \theta U_e/\nu$ and the friction Reynolds number is defined as $Re_\tau = \delta_{99} u_\tau/\nu$ ($u_\tau = \sqrt{\tau_w/\rho}$). Note that the choice of different ranges of Re_θ between the ZPG and APG TBL over the flate plate is a direct consequence of the different pressure-gradient conditions. In particular, a positive value of β results in a higher θ and thus higher Re_θ. A similar effect is also observed for uniform blowing, in the comparison between reference (WSS) and controlled (WSSB) wing simulation. The behaviour of the friction Reynolds number, on the other hand, is more complex, because APG and uniform blowing increase the boundary-layer thickness but also reduce friction at the same time. In the flat-plate cases considered here, the net effect of the pressure gradient is that of increasing Re_τ, but on the suction side of the wing, at very high values of β (Vinuesa *et al.*, 2018) or in the case of blowing (Atzori *et al.*, 2021), Re_τ eventually decreases. Due to this effect, Re_τ cannot be considered a reliable indicator of scale separation in cases with intense APGs.

SKIN-FRICTION CONTRIBUTIONS

The FIK identity is derived from the mean-momentum conservation in the wall-tangential direction, which can be written in conservative form as:

$$\frac{\partial(U^2)}{\partial x} + \frac{\partial(UV)}{\partial y} = -\frac{\partial P}{\partial x} + \nu\left(\frac{\partial^2 U}{\partial y^2} + \frac{\partial^2 U}{\partial x^2}\right) + \frac{\partial \overline{uv}}{\partial y} + \frac{\partial \overline{u^2}}{\partial x}. \tag{1}$$

In this expression, $U = U_t$ and $V = V_n$ denote the wall-tangential and wall-normal mean velocity components, respectively, and $x = x_t$ and $y = y_n$ denote the wall-tangential and wall-normal coordinates, respectively. Note that we will focus on cases where wall-curvature effects are absent or negligible. Applying a triple integration by parts to Eq. (1), one can obtain: $c_f = c_f^\delta + c_f^T + c_f^D + c_f^P$. In this expression, $c_f^\delta = 4(1-\delta_{99}/\delta^*)/Re_\delta$ denotes a contribution directly related to the boundary-layer thickness (where $Re_\delta = U_e\delta_{99}/\nu$); $c_f^T = -4\int_0^1 \int (1-\eta)\overline{uv}\,\mathrm{d}\eta$ is the turbulent-fluctuation contribution; $c_f^P = -2\int_0^1 (1-\eta)^2(\partial P/\partial x)\,\mathrm{d}\eta$ is the contribution that includes the pressure gradient; and $c_f^D = -2\int_0^1 (1-\eta)^2 I_x\,\mathrm{d}\eta$ includes the remaining terms of Eq. (1), which are zero for flows that are homogeneous in the wall-tangential direction, *i.e.*:

$$I_x = \frac{\partial(U^2)}{\partial x} + \frac{\partial(\overline{u^2})}{\partial x} + \frac{\partial(UV)}{\partial y} - \frac{1}{Re_\delta}\frac{\partial^2 U}{\partial x^2}. \tag{2}$$

The integration variable, $\eta = y/\delta_{99}$ is the wall-normal coordinate normalised with the boundary-layer thickness. The contribution c_f^D can be further decomposed into four terms: $c_f^D = c_f^{D1} + c_f^{D2} + c_f^{D3} + c_f^{D4}$. These four additional contributions correspond to the four terms included in I_x, for instance $c_f^{D1} = -2\int_0^1 (1-\eta)^2(\partial U^2/\partial x)\,\mathrm{d}\eta$.

The first two contributions, c_f^{D1} and c_f^{D2}, are directly related to the flow development in the wall-tangential direction; c_f^{D3} is related to mean wall-normal convection; and c_f^{D4} is related to viscous dissipation due to streamwise inhomogeneity. These four terms are not of the same order of magnitude because c_f^{D1} and c_f^{D3} tend to be much larger then c_f^{D2} and c_f^{D4}, so that their balance determines the streamwise development of c_f^D.

An alternative form of the skin-friction contributions can be obtained if the triple integration by parts is performed on the convective form of Eq. (1). In this case, the inhomogeneity term I_x becomes:

$$I_x^* = U\frac{\partial U}{\partial x} + \frac{\partial(\overline{u^2})}{\partial x} + V\frac{\partial U}{\partial y} - \frac{1}{Re_\delta}\frac{\partial^2 U}{\partial x^2}. \tag{3}$$

This formulation leads to different contributions related the mean convection, denoted by c_f^{D1*} and c_f^{D3*}, instead of c_f^{D1} and c_f^{D3}. The definitions of c_f^{D1*} and c_f^{D3*} suggest that it is possible to rearrange the contributions in the following way.

In the irrotational region above the boundary layer, the Bernoulli and Euler equations (approximately) hold:

$$\frac{1}{2}U^2 + P = P_0 \quad \Rightarrow \quad U\frac{\partial U}{\partial x} = -\frac{\partial P}{\partial x}, \tag{4}$$

where $q = (1/2)U^2$ is the dynamic pressure, and the total pressure, denoted by P_0, is constant. The same expression is also obtained in the context of the boundary-layer approximation, and it shows a connection between c_f^{D1*} and c_f^P. We then define two new contributions as:

$$c_f^{DP} = c_f^{D1*} + c_f^P = -2\int_0^1 (1-\eta)^2\left(U\frac{\partial U}{\partial x} + \frac{\partial P}{\partial x}\right)\mathrm{d}\eta, \tag{5}$$

$$c_f^{DV} = c_f^{D3*} = -2\int_0^1 (1-\eta)^2 V\frac{\partial U}{\partial \eta}\,\mathrm{d}\eta. \tag{6}$$

The first one can be written in terms of the contributions derived from the conservative form as $c_f^{DP} = (1/2)c_f^{D1} + c_f^P$, while the latter can be written as $c_f^{DV} = (1/2)c_f^{D1} + c_f^{D3}$.

The sign of the c_f^{DP} contribution shows in which direction the turbulent boundary layer departs from the conditions under which the Bernoulli equation holds. Note that we will

focus on APG TBLs, where $\partial P/\partial x > 0$. In the free stream, the integrand of c_f^{DP} is zero. In the case that $U(\partial U/\partial x) > \partial P/\partial x$, *i.e.* the rate of change in the streamwise direction of the dynamic pressure is higher than in a corresponding irrotational flow, c_f^{DP} is negative, leading to skin friction reduction. On the other hand, if $U(\partial U/\partial x) < \partial P/\partial x$, *i.e.* the rate of change of the dynamic pressure is lower than in a corresponding irrotational flow, then c_f^{DP} is positive. Note that these inequalities do not necessary hold at every wall-normal distance because of the integration along η, but are indications of the general trend.

The contribution that includes the wall-normal convection, c_f^{DV}, can be further decomposed by introducing the mean spanwise vorticity (denoted by $\Omega_z = \partial V/\partial x - \partial U/\partial y$): $c_f^{DV} = c_f^{DVV} + c_f^{D\Omega}$. The first and second term in this expression include $V(\partial V/\partial x)$ and $-V\Omega_z$, respectively:

$$c_f^{DVV} = -2\int_0^1 (1-\eta)^2 \left(V\frac{\partial V}{\partial x}\right) \mathrm{d}\eta, \tag{7}$$

$$c_f^{D\Omega} = +2\int_0^1 (1-\eta)^2 V\Omega_z \,\mathrm{d}\eta. \tag{8}$$

The introduction of these new terms is motivated by the fact that $\partial U/\partial y$ tends to be much larger than $\partial V/\partial x$ in TBLs, so that c_f^{DVV} is negligible and c_f^{DV} can be approximated with $c_f^{D\Omega}$ in most cases. Assuming that V is positive, the sign of $c_f^{D\Omega}$ is negative. The sign of $c_f^{D\Omega}$ shows that wall-normal convection is always associated with skin-friction reduction, which is a natural consequence of the fact that it reduces near-wall momentum.

RESULTS

In the present section, we will examine contributions to the skin friction, as evaluated from the two formulations of the FIK identity discussed above. Our objective is to illustrate how the convective formulation is more sensitive to the streamwise development of the flow than the conservative one, and more effective in highlighting the relevant contributions. Later on, the more detailed information obtained with the new formulation is used to discuss how increasingly intense APGs may lead to separation.

Flat-plate boundary layers

We first consider the ZPG TBL at friction Reynolds numbers between $Re_\tau \approx 200$ and 570, and the two APG TBLs at similar Re_τ but under different pressure-gradient conditions, as shown in Fig. 1. In this figure, we focus on the most relevant relative FIK contributions, which are normalised with the total c_f. In the ZPG TBL, relative skin-friction contributions exhibit only a weak dependence on the Reynolds number as x increases. The turbulent term is the most relevant one, and maintains a value of $c_f^T \approx 70\% c_f$ (values at $x = 750$ are reported in Fig. 2). If the conservative FIK formulation is used, c_f^P vanishes, but the two contributions including the mean velocity components have still magnitudes of $c_f^{D1} \approx 48\% c_f$ and $c_f^{D3} \approx -28\% c_f$. If the convective formulation is used, the contribution $c_f^{D\Omega}$ is negligible, and this result immediately shows the limited relevance of wall-normal convection in the ZPG case. At the same time, $c_f^{DP} \approx 24\% c_f$ so that the change of dynamic pressure is identified as the dominant inhomogeneity contribution. The positive sign of c_f^{DP} also shows that the dynamic pressure is decreasing faster within the turbulent boundary layer than in a corresponding irrotational flow.

APG TBLs exhibit a more complex behavior and c_f^P, c_f^{D1}, and c_f^{D3} have absolute values much higher than c_f. The balance between these terms is not obvious, at a first sight. In fact, c_f^{D1} is positive while c_f^P and c_f^{D3} are negative, and they all become rapidly more relevant in terms of relative contribution to c_f as β increases. Because all terms connected to streamwise inhomogeneity have similar evolution, it is not possible to readily distinguish different regimes for the various values of β. The high magnitude of these contributions also suggests the counter-intuitive conclusion that turbulent fluctuations play a only minor role in determining friction, further highlighting the necessity of re-grouping different terms.

If the convective formulation is used, c_f^T becomes the most relevant contribution. Comparing its absolute magnitude in APG and ZPG (not shown here), c_f^T is even higher in APG than in ZPG TBLs at similar Re_θ or Re_τ, despite the lower c_f in the former. This fact is due to the intense turbulent fluctuations in the outer region of the APG TBLs. Both dynamic-pressure and vorticity-convection contributions have lower intensities than c_f^T, contrary to the inhomogeneity contributions of the conservative FIK formulation. The dynamic-pressure contribution c_f^{DP} describes directly the balance between c_f^P and c_f^{D1}, and the contribution $c_f^{D\Omega}$ is always negative and rapidly becomes smaller in the region of quickly-increasing β, but later increases (*i.e.* its modulus decreases, thus approaching zero from negative values). The streamwise development of c_f^{DP} and $c_f^{D\Omega}$ allows to identify different streamwise regions, corresponding to changes in the development of the Clauser pressure-gradient parameter β and the total c_f. At low values of β, c_f^{DP} is in good agreement between APG and ZPG. As β continues to increase, c_f^{DP} decreases up to changing sign and it eventually reaches an equilibrium value if β is approximately constant for a portion of the domain that is long enough. The change of sign of c_f^{DP} happens to be at a similar location as the maximum value of β (which is the location examined in Table 2). Note that the vorticity-convection contribution is immediately affected by the change of β, causing the decrease of c_f in the first portion of the flat plate. Only downstream, the dynamic-pressure contribution also contributes to reducing c_f. The sign of c_f^{DP} shows that the TBL is moving from a state where the dynamic pressure is increasing at a lower rate than for a corresponding irrotational flow, to a state where the dynamic pressure is increasing at a higher rate.

An interesting observation is possible from both FIK formulations, which is that a significant change of state of the boundary layer occurs not as a result of β reaching its maximum value, but rather as a results of the change of rate at which β is increasing before reaching its maximum, at a lower x. For both β distributions, the relative contributions due to convection peak before the maximum β, where c_f is rapidly decreasing as compared to the ZPG case. The relative contributions later decrease and, at much higher x, where β is almost uniform and decreasing, they eventually reach a more stable values. The conservative formulation provides a precise description of the transitional regime between these two states, which is captured by c_f^{DV}. The relatively long transition between the two states that appears in Fig. 1, compared with the β distribution, is another facet of history effects (Bobke *et al.*, 2017).

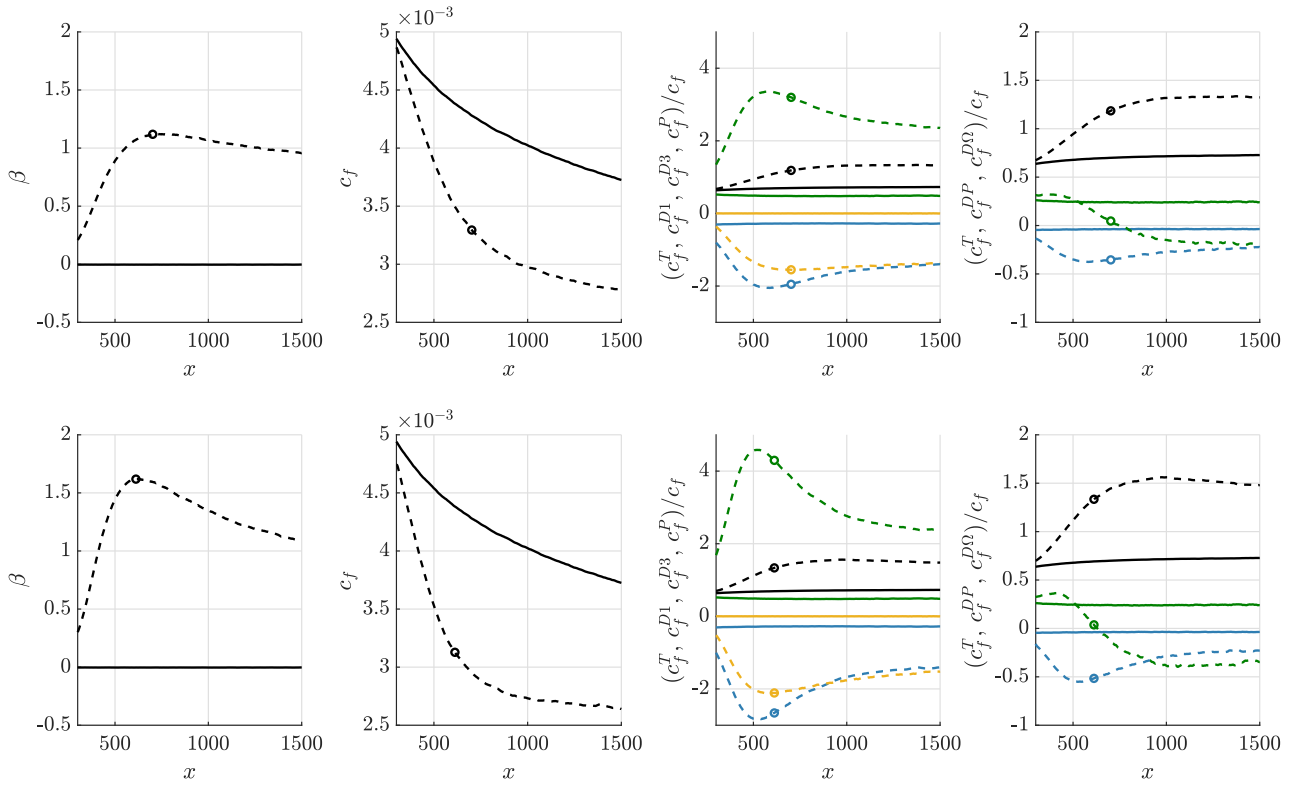

Figure 1. Comparison between ZPG and (top row) APG1 and (bottom row) APG2. Solid and dashed lines denote the ZPG and APG data, respectively. (Left column) Clauser pressure-gradient parameter, denoted by β. (Center-left column) Skin-friction coefficient, denoted by c_f. (Center-right column) Relative skin-friction contributions from the conservative formulation: (■, c_f^T/c_f) turbulent fluctuations, (■, c_f^{D1}/c_f) mean-velocity streamwise-development, (■, c_f^{D3}/c_f) mean wall-normal convection of momentum, and (■, c_f^P/c_f) pressure-gradient. (Right column) Relative skin-friction contributions from the convective formulation: (■, c_f^T/c_f) turbulent fluctuations, (■, c_f^{DP}/c_f) dynamic pressure, and (■, $c_f^{D\Omega}/c_f$) mean wall-normal convection of vorticity. The turbulent-fluctuation contribution is the same in both the center-right and right columns. Note that $c_f^{DP} = 1/2c_f^{D1} + c_f^P$ and $c_f^{DV} = 1/2c_f^{D1} + c_f^{D3}$. The circles denote the location with highest β. Notice the different scales in the right-hand panels.

Table 2. Relative skin-friction contributions at a selected location for the ZPG, APG1, and APG2. For the APG1 and APG2, the values are at the location of maximum β (highlighted in Fig. 1). For the ZPG, at $x = 750$. The red square denote the most intense relative contribution or relative control effect.

FIK (conservative formulation)				**FIK (convective formulation)**			
	ZPG	APG1	APG2		ZPG	APG1	APG2
c_f^T/c_f(■)	70%	118%	133%	c_f^T/c_f(■)	70%	118%	133%
c_f^{D1}/c_f(■)	48%	320%	429%	c_f^{DP}/c_f(■)	24%	5%	4%
c_f^{D3}/c_f(■)	−28%	−195%	−266%	$c_f^{D\Omega}/c_f$(■)	−4%	−36%	−52%
c_f^P/c_f(■)	0%	−155%	−211%	$(c_f^\delta + c_f^{D2} +$	10%	13%	15%
$(c_f^\delta + c_f^{D2} + c_f^{D4})/c_f$	10%	12%	15%	$+ c_f^{D4} + c_f^{DVV})/c_f$			
Total	100%	100%	100%	Total	100%	100%	100%

Wing boundary layers and control effects

A qualitative difference between how both FIK formulations describe pressure-gradient effects is also evident in the identification of the most relevant contribution in TBL developing over the NACA4412 suction side (Figs. 2 and 3).

Due to the relatively high values of the pressure gradient and the mean-velocity components, turbulent fluctuations appear again to have a secondary role in determining the value of the total c_f, if the conservative formulation is employed. The cause for decreasing c_f is also not directly evident because the three highest contributions, c_f^T, c_f^{D1}, and c_f^{D3}, have all a similar streamwise development and are much larger than c_f. For instance, c_f^{D1} reaches a value of more than 9 times the total c_f at $x/c = 0.75$ (Fig 3), and even higher values further downstream.

On the other hand, if the convective formulation is used, c_f^T becomes the skin-friction contribution with highest absolute value over most of the profile, up to the region of very strong APG at $x \approx 0.8$. In this case, c_f^{DP} is always positive and follows the development of β. Subsequently, the decrease of c_f, which would eventually lead to separation for a higher angle of attack, is entirely due to the enhanced vorticity convection in the wall-normal direction. This phenomenon is not directly evident when the conservative FIK formulation is considered.

The streamwise development of the relative contributions on the airfoil highlights similarities with the first portion of

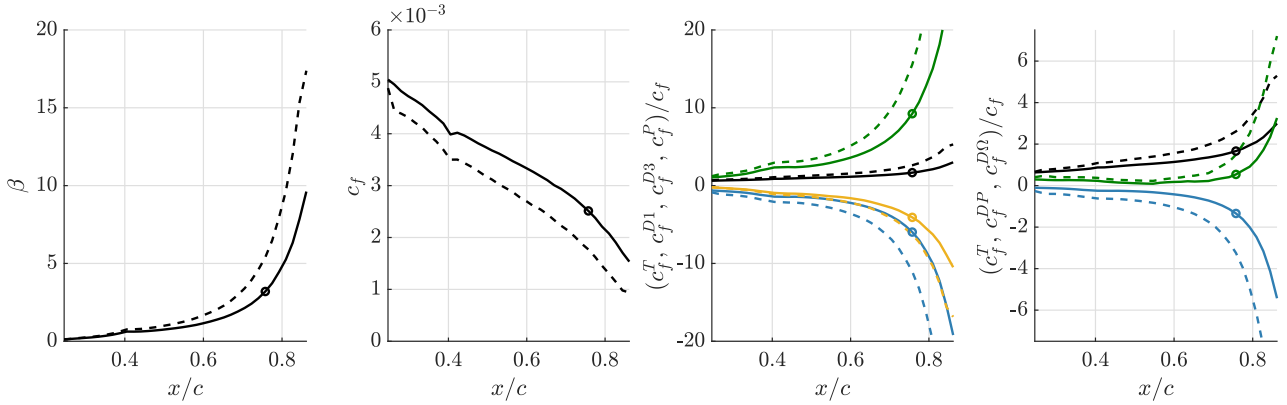

Figure 2. Comparison between (solid lines) suction side of a NACA4412 at $Re_c = 400,000$, and (dashed lines) the same case with uniform blowing. Color code for skin-friction contributions as in Fig. 1. The circles denote the streamwise location $x/c = 0.75$.

Table 3. Skin-friction contributions and control effects normalised with the total c_f at $x/c = 0.75$ on suction side of the airfoil, at the location highlighted in Fig. 2. The red squares denote the most intense relative contribution or relative control effect.

FIK (conservative formulation)				**FIK (convective formulation)**			
Reference case		Blowing effects		Reference case		Blowing effects	
c_f^T/c_f(■)	167%	$\Delta c_f^T/c_f$(■)	+17%	c_f^T/c_f(■)	167%	$\Delta c_f^T/c_f$(■)	+17%
c_f^{D1}/c_f(■)	924%	$\Delta c_f^{D1}/c_f$(■)	+172%	c_f^{DP}/c_f(■)	54%	$\Delta c_f^{DP}/c_f$(■)	+51%
c_f^{D3}/c_f(■)	−597%	$\Delta c_f^{D3}/c_f$(■)	−180%	$c_f^{D\Omega}/c_f$(■)	−134%	$\Delta c_f^{D\Omega}/c_f$(■)	−94%
c_f^P/c_f(■)	−408%	$\Delta c_f^P/c_f$(■)	−35%	$(c_f^\delta + c_f^{D2} +$	13%	$(\Delta c_f^\delta + \Delta c_f^{D2} +$	−3%
$(c_f^\delta + c_f^{D2} + c_f^{D4})/c_f$	14%	$(\Delta c_f^\delta + \Delta c_f^{D2} + \Delta c_f^{D4})/c_f$	−3%	$+ c_f^{D4} + c_f^{DVV})/c_f$		$+ \Delta c_f^{D4} + \Delta c_f^{DVV})/c_f$	
Total	100%	Total $\Delta c_f/c_f$	−29%	Total	100%	Total $\Delta c_f/c_f$	−29%

the flat plate, where β is also rapidly increasing. In particular, c_f^{DP}/c_f is positive and $c_f^{D\Omega}/c_f$ becomes progressively lower. However, contrary to the flat-plate cases, β is increasing over the entire streamwise extent, eventually leading to both c_f^{DP} and $c_f^{D\Omega}$ having a higher absolute value than c_f^T, which was not observed for the flat plate, where β does not increase fast enough and for a long enough portion of the domain. These observations were not obvious using the conservative FIK formulation, due to the high values of all terms, which makes more difficult to distinguish different state of the boundary layer.

The new FIK formulation also simplifies the description of control effects, here discussed in terms of control using wall transpiration. In fact, uniform blowing is known to reduce skin friction and has non-linear interactions with APG (see e.g. Eto *et al.*, 2019; Atzori *et al.*, 2021). Applying the FIK decomposition, blowing significantly increases c_f^T and c_f^{D3}, and decreases c_f^{D1} and c_f^P. In particular, c_f^{D1} and c_f^{D3} are increased and decreased, respectively, by an amount which is almost equal to $2c_f$. However, the modifications of c_f^{DP} and $c_f^{D\Omega}$ are less dramatic, so that the conservative formulation allows to identify immediately that the skin-friction reduction is due to the increased mean-vorticity convection, which counterbalances the increase of dynamic-pressure and turbulent contributions.

Path towards separation

In principle, the onset of mean separation, corresponding to $c_f = 0$, can be approached from any combination of relative contributions. In the particular case in which all terms decrease at the same rate, c_f will also decrease accordingly. This is what we observed in the ZPG case, where the relative contributions are approximately constant, despite the gentle reduction of c_f due to the boundary-layer development in near-equilibrium conditions Bobke *et al.* (2017). On the other hand, if c_f is obtained as a result of cancellation of terms with opposite sign and changing at different rates, the corresponding relative contributions will progressively increase. In fact, contributions that are decreasing slower than c_f or increasing will virtually diverge at $c_f = 0$. Under the conditions of adverse pressure gradient, the c_f reduction is indeed the result of a change of absolute as well as relative skin-friction contributions, *i.e.* a modification of how different phenomena concur in determining the total friction. In particular, we identified three different regimes: 1) rapidly increasing values of β, where c_f^{DP} is positive and increasing but $c_f^{D\Omega}$ is decreasing (*i.e.* becoming more negative) faster than c_f^{DP} increases, leading to a rapid reduction of c_f; 2) decreasing values of β, where both c_f^{DP} and $c_f^{D\Omega}$ are negative but with approximately constant relative contributions, associated with a slow reduction of c_f; and 3) an intermediate region, with values of β that are either slowly increasing or decreasing, where c_f^{DP} and $c_f^{D\Omega}$ tend to decrease and increase, respectively, towards their values in regime 2).

The similarities between the second regime and the ZPG case suggest that mean separation will not occur under these conditions. The data extracted from the wing boundary layer, on the other hand, suggest that separation will occur in a state similar to that of the first regime. We can thus formulate the hypothesis that in the specific case considered here, namely β increasing from a low value as the boundary layer develops, there exists a critical rate of change of β above which the adverse pressure gradient will eventually cause separation, and below which separation will not occur. This hypothesis is also corroborated by the fact that turbulent boundary layers at higher Reynolds number are less sensitive to pressure gradients. There is thus a distinction between a TBL that is leading

towards separation, where the rate at which β is increasing is fast enough to overcome the growth of the boundary layer, and the opposite case where, even though β remains positive and still increasing, the boundary layer approaches a state progressively farther from separation.

Key questions to address in this description of the path towards separation remain: 1) whether it is actually enough to observe the onset of the intermediate regime, to determine that separation will not occur, and 2) what is the impact of the initial value of β. In fact, in cases such as that of an initially very high but constant or even decreasing β, the increase of Reynolds number may not be enough to avoid separation.

CONCLUSIONS AND OUTLOOK

We described a new formulation of FIK skin-friction decomposition with contributions that are related to streamwise inhomogeneity, and we discussed how the results of the decomposition change in TBLs subjected to various pressure-gradient conditions, including one flow-control case with uniform blowing. The new formulation is derived from the convective form of the mean streamwise momentum conservation, and the concept of dynamic pressure is used to re-group the pressure gradient and wall-tangential derivatives. The implicit cancellations in the definition of the new dynamic-pressure and vorticity-convection contributions allow these two terms to be more sensitive to pressure-gradient conditions, and to identify immediately the main phenomena that govern the development of c_f. In particular, the new formulation distinguishes more easily between adverse-pressure gradients of different intensities, and between mean-flow and turbulent-fluctuations effects.

We identified that APGs can lead to different states of the boundary layers, depending on the flow history as well as the value and the local rate of the change of the pressure-gradient parameter, β. Intense and quickly-increasing β leads to a regime where the dynamic-pressure contribution is positive and increasing, but such an increase is counteracted by the fast decrease of the vorticity-convection contribution, resulting in a fast reduction of c_f and eventually to separation. A uniform or decreasing β instead, causes both dynamic-pressure and vorticity-convection contributions to be negative but almost uniform, resulting in a lower reduction rate for c_f. This regime is in fact similar to that of a ZPG TBL. The trends observed on flat-plate and wing TBLs suggested that it is possible to employ the skin-friction contributions to study how APGs lead to separation. Finally, this study confirm once again the importance of history effects in determining the local state of the flow, as clearly shown by the postponed evolution of the skin-friction contributions, with respect to that of β.

A few consideration are left for future studies. Our results suggest that the rate of the change of β is critical in determining whether a progressively stronger adverse pressure gradient can cause separation, and that the state of the flow that precedes separation is characterised by specific rates of change of the relative contributions. It may be worth to further develop these ideas, examining a larger sample of data. A refined derivation of the new formulation of FIK identity will be also considered, to highlight curvature effects. A similar aggregation between contributions may also be introduced in the RD decomposition (Renard & Deck, 2016).

REFERENCES

Atzori, M., Vinuesa, R., Stroh, A., Gatti, D., Frohnapfel, B. & Schlatter, P. 2021 Uniform blowing and suction applied to non-uniform adverse-pressure-gradient wing boundary layers. *Phys. Rev. Fluids* **6**, 113904.

Bobke, A., Vinuesa, R., Örlü, R. & Schlatter, P. 2017 History effects and near-equilibrium in adverse-pressure-gradient turbulent boundary layers. *J. Fluid Mech.* **820**, 667–692.

Chevalier, M., Schlatter, P., Lundbladh, A. & Henningson, D.S. 2007 A Pseudo-Spectral Solver for Incompressible Boundary Layer Flow. Tech. Rep. TRITA-MEK 2007:07, Royal Institute of Technology, Stockholm, Sweden.

Clauser, F. 1956 The turbulent boundary layer. *Adv. Appl. Mech.* **4**, 1–51.

Eitel-Amor, G., Örlü, R. & Schlatter, P. 2014 Simulation and validation of a spatially evolving turbulent boundary layer up to $Re_\theta = 8300$. *Int. J. Heat Fluid Flow* **47**, 57–69.

Eto, K., Kondo, Y., Fukagata, K. & Tokugawa, N. 2019 Assessment of friction drag reduction on a Clark-Y airfoil by uniform blowing. *AIAA J.* **57** (7), 2774–2782.

Fan, Y., Atzori, M., Vinuesa, R., Gatti, D., Schlatter, P. & Li, W. 2022 Decomposition of the mean friction drag on an naca4412 airfoil under uniform blowing/suction. *J. Fluid Mech.* **932**, A31.

Fischer, P.F., Kruse, J., Mullen, J., Tufo, H., Lottes, J. & Kerkemeier, S. 2008 Nek5000: open source spectral element cfd solver. Available at `http://nek5000.mcs.anl.gov/`.

Fukagata, K., Iwamoto, K. & N., Kasagi. 2002 Contribution of Reynolds stress distribution to the skin friction in wall-bounded flows. *Phys. Fluids* **14**, L73–L76.

Kametani, Y., Fukagata, K., Örlü, R. & Schlatter, P. 2015 Effect of uniform blowing/suction in a turbulent boundary layer at moderate Reynolds number. *Int. J. Heat Fluid Flow* **55**, 134–142.

Renard, N. & Deck, S. 2016 A theoretical decomposition of mean skin friction generation into physical phenomena across the boundary layer. *J. Fluid Mech.* **790**, 339–367.

Schlatter, P., Stolz, S. & Kleiser, L. 2004 LES of transitional flows using the approximate deconvolution model. *Int. J. Heat Fluid Flow* **25**, 549–558.

Vinuesa, R., Bobke, A., Örlü, R. & Schlatter, P. 2016 On determining characteristic length scales in pressure-gradient turbulent boundary layers. *Phys. Fluids* **28**, 055101.

Vinuesa, R., Negi, P.S., Atzori, M., Hanifi, A., Henningson, D.S. & Schlatter, P. 2018 Turbulent boundary layers around wing sections up to $Re_c = 1,000,000$. *Int. J. Heat Fluid Flow* **72**, 86–99.